LAWRENCE
LIVERMORE
NATIONAL
LABORATORY

LLNL-CONF-406817

Dilepton-Tagged Q-Qbar+Jet Events at the LHC

C. Mironov, R. Vogt, G. J. Kunde

September 5, 2008

Hard Probes 2008
Illa de A Toxa, Spain
June 9, 2008 through June 14, 2008

Disclaimer

EPJ manuscript No.
(will be inserted by the editor)

Dilepton-Tagged $Q\overline{Q}$+Jet Events at the LHC

Camelia Mironov[1], Ramona Vogt[2], and Gerd J. Kunde[1]

[1] Los Alamos National Laboratory, PO Box 1663 Los Alamos, NM USA
[2] Lawrence Livermore National Laboratory and UC Davis

Received: date / Revised version: date

Abstract. We propose a new method for identifying and isolating $Q\overline{Q}$+jet events through semileptonic decays of the $Q\overline{Q}$ pair. Employing these decay dileptons to tag the jet in a specific kinematic region provides a clean signature of jets associated with heavy quark production. The measurement, in both pp and heavy-ion collisions, is essential for addressing heavy quark fragmentation in the vacuum and in a dense medium. We present next-to-leading order calculations of $Q\overline{Q}$ production (leading order in $Q\overline{Q}$+jet production) in $\sqrt{s} = 14$ TeV pp collisions at the LHC and discuss the feasibility of the measurement in heavy-ion collisions at $\sqrt{s_{NN}} = 5.5$ TeV.

PACS. 13.87.Ce jet production – 24.85.+p QCD in nuclear reactions – 25.75.Cj heavy quark production in rel. HI colls – 12.38.Qk experimental tests of QCD

1 Introduction

Heavy quarks are important probes of QCD production and hadronization in both fundamental pp collisions and ultrarelativistic heavy-ion collisions. They are calculationally attractive because their large mass makes it possible to obtain the production rate over the entire p_T range. Therefore, accurate heavy quark measurements provide direct quantitative tests of QCD, including a detailed understanding of their production, fragmentation and evolution. Since heavy quarks constitute an important part of the background to many new particle searches in the Large Hadron Collider (LHC) pp program [1], detailed knowledge of their properties is vital. In heavy-ion collisions, because the heavy quark production time, $\sim 1/2m_Q \simeq 0.3$ fm for $m_c = 1.5$ GeV/$c2$ and 0.1 fm for $m_b = 4.75$ GeV/$c2$, is short compared to the ~ 1 fm formation time of a quark-gluon plasma, heavy quarks experience the full collision history. Thus heavy flavor observables probe both production and propagation through the medium.

Jets are another key high p_T and high $Q2$ QCD probe of hard production and fragmentation. Jet measurements will be an important component of the LHC pp and heavy-ion programs.

The high energy and luminosity LHC is the ideal environment for studies of both jets and heavy-quark production. The large LHC detectors (CMS [2], ATLAS [3], and ALICE [4]), with wide calorimetric coverage and high-resolution tracking, can identify jets using standard reconstruction methods (*e.g.* jet algorithms that reconstruct the jet energy deposited in the calorimeters as well as momentum and angular hadron correlation methods that access jet properties on a statistical basis) over a wide rapidity range. Particle identification (to reconstruct hadronic decays), together with high-quality tracking and fine vertex-reconstruction capabilities and extended lepton coverage (for lepton identification and displaced-vertex analysis of semileptonic decays) are available for heavy-flavor detection. However, disentangling the signal from the enormous background, leaving similar signatures in the detectors, is still challenging.

We propose a heavy-flavor measurement that combines heavy flavor and jet probes. Next-to-leading order (NLO) calculations of heavy-quark production predicts final states with three hard, correlated partons such as $Q\overline{Q}g$ and $Q\overline{Q}q$. The resulting $Q\overline{Q}$+jet events should provide a unique high p_T and large $Q2$ test of QCD. The $Q\overline{Q}$ pairs are identified by their decays to lepton pairs, dominating the dilepton continuum above the Υ mass. These high mass, heavy-flavor decay dileptons are used to tag jets. Our results, presented for $\sqrt{s} = 14$ TeV pp collisions, include acceptance cuts appropriate for the three large LHC detectors. We also briefly comment on measurements in the more challenging environment of Pb+Pb collisions at $\sqrt{s_{NN}} = 5.5$ TeV.

With a pure sample of heavy quark decay products, it is possible to study the heavy quark fragmentation function (FF). In general, the FFs, assumed to be universal, are determined from e^+e^- measurements. Data from different center-of-mass energies are employed to obtain their $Q2$ evolution. However, despite the wide range of e^+e^- data, it is not yet possible to determine the existence and nature of the power corrections to the fragmentation functions [5] and represents one of the largest sources of uncertainty in the high p_T heavy flavor production cross section [6]. It is thus important to develop new tools for

probing the heavy flavor fragmentation functions in the new kinematical regime of the LHC, even in *pp* collisions.

In the environment of a heavy-ion collision, the baseline heavy quark vacuum FFs are expected to be modified. The study of these predicted modifications is therefore an important means of determining the properties of high-density QCD matter. Further, multiplicity-dependent 'tomography' of Q and $\overline{Q}$ jets as a function of momentum and cone size, directly related to gluon bremsstrahlung by the heavy quarks while passing through the dense medium, will address heavy-quark energy loss [7]. While heavy quarks are expected to lose less energy than light quarks due to their larger mass, the RHIC data so far on non-photonic electron spectra suggest that this may not be the case [8]. Since the electrons have not been unambiguously determined to be from heavy flavor decays, the strength of the energy loss effects on charm and bottom quarks remains unknown. Our method could help clarify the situation.

Finally, the $Q\overline{Q}$+jet topology can shed light on the heavy quark production mechanism. In particular, the clean environment of *pp* collisions at the LHC and the excellent lepton identification of the detectors probe the relative importance of two- to three-body final states at high p_T.

2 Calculational Method

Heavy quark production has been calculated at NLO using the exclusive $Q\overline{Q}$ code of Mangano, Nason and Ridolfi [9], HVQMNR. The leading order (LO) contributions to heavy quark production are gluon fusion, $g + g \rightarrow Q + \overline{Q}$, and quark-antiquark annihilation, $q + \overline{q} \rightarrow Q + \overline{Q}$. At NLO, a third hard parton can be produced in the final state, leading to $Q\overline{Q}$+jet events from both gg and $q\overline{q}$ initial states, as well as $q + g \rightarrow q + Q + \overline{Q}$ processes. The parameters used in HVQMNR are listed in Table 1.

Table 1. The HVQMNR parameters: $\langle k_T \rangle$ is the mean intrinsic transverse momentum; ϵ is the parameter in the Peterson function [10]; ξ_F and ξ_R are the ratios of the factorization and renormalization scales relative to the quark transverse mass, m_T. The CTEQ6M parton densities [11] are used.

Q	m_Q (GeV/c^2)	$\langle k_T \rangle$ (GeV/c)	ϵ	ξ_F	ξ_R
c	1.5	1.0	0.06	1.0	1.0
b	4.75	1.0	0.006	1.0	1.0

We use the Peterson fragmentation function [10], the HVQMNR default. The Peterson function reduces the charm quark momentum 30% on average during fragmentation while the bottom quark momentum is reduced by 10%.

The semileptonic decay branching ratios we use are $D \rightarrow lX$ (10.3%) and $B \rightarrow lX$ (10.86%) for $l = e$ and μ. These branching ratios are averages for generic D and B mesons. The implementation of B decays in HVQMNR is described in Ref. [12]. The D decays employ a similar technique.

Four sets of dilepton kinematic cuts, outlined in Table 2, were considered. The cuts were chosen taking the single lepton identification capabilities of the LHC experiments [2–4], into accouunt. The single lepton cuts are determined by the minimum lepton p_T and maximum η coverage of the ALICE (Cut_1) and CMS (Cut_2-Cut_4) detectors. The lower limit on the dilepton p_T is chosen by considering that, for typical light hadron fragmentation, $\approx 20\%$ of the final-state light parton p_T (in the $Q\overline{Q}X$ final state where X is a light quark or gluon) is carried by the leading hadron (the hadron in the jet with the highest p_T). Thus a parton with $p_T \sim 25$ GeV/c will produce a leading hadron with $\langle p_T \rangle \sim 5$ GeV/c. Therefore, a sufficiently high dilepton p_T cut will ensure that the jet is observable over the hadronic background. Also, previous studies [13] showed that intrinsic k_T effects are more pronounced at lower hadron p_T, making the results harder to interpret.

Table 2. Single lepton and dilepton cuts. Cut_1 represents the ALICE electron identification capabilities. The CMS muon coverage is assumed for Cut_2 and Cut_3 while Cut_4 is a mixed $e\mu$ cut in CMS.

Observable	Cut_1	Cut_2	Cut_3	Cut_4
M (GeV/c^2)	[12,70]	[12,70]	[12,70]	None
$p_{T\,1}^{l\,\mathrm{min}}$ (GeV/c)	1.0	3.5	3.5	3.5
$\lvert\eta_1^{l\,\mathrm{max}}\rvert$	0.9	2.4	2.4	2.4
$p_{T\,2}^{l\,\mathrm{min}}$ (GeV/c)	1.0	3.5	3.5	5.0
$\lvert\eta_2^{l\,\mathrm{max}}\rvert$	0.9	2.4	2.4	3.0
p_T^{min} (GeV/c)	5.0	10.0	25.0	25.0

3 $Q\overline{Q}$ tagged jets

We will focus on the dilepton invariant mass region $12 < M < 70$ GeV/c^2, below the Z^0 peak but above the Υ states, where $Q\overline{Q} \rightarrow l^+l^-X$ dominates the signal dileptons. The main physics channels contributing to the signal in this mass range are virtual photons ($\gamma^* \rightarrow l^+l^-$) and correlated semileptonic $D\overline{D}$ and $B\overline{B}$ decays. The mass distributions for all three cases are shown in Fig. 1. The heavy flavor decays clearly dominate in the region between the Υ and Z^0 peaks.

Since $Q\overline{Q}$ pairs can be accompanied by a quark or a gluon jet at NLO, we develop a way to identify and measure the $Q\overline{Q}$+jet signal. We show that an azimuthal cut between the leptons from semileptonic heavy flavor decays can help isolate the $Q\overline{Q}$+jet topologies.

3.1 Heavy Quarks

In Fig. 2, the individual LO (open symbols) and NLO (full symbols) contributions to the dilepton p_T distribution from the initial $q\overline{q}$, gg and qg channels are shown. The only kinematic cut is on the $Q\overline{Q}$ pair mass: $12 < M < 70$

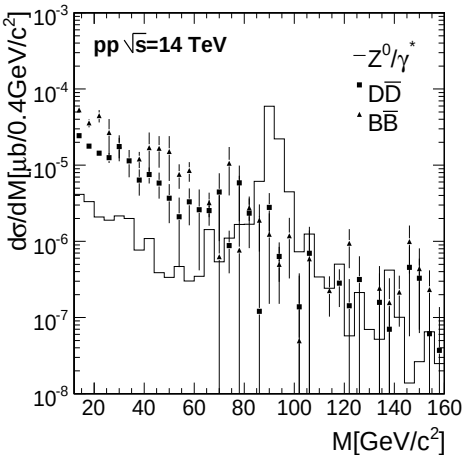

Fig. 1. Dilepton invariant mass distributions from $D\overline{D}$ and $B\overline{B}$ semileptonic decays and $Z^0/\gamma^* \to l^+l^-$ in pp collisions at $\sqrt{s} = 14\,\mathrm{TeV}$.

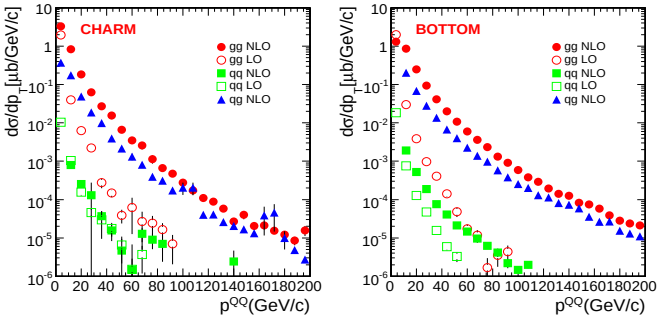

Fig. 2. The partonic contributions to the $c\bar{c}$ (left) and $b\bar{b}$ pair (right) p_T in the mass interval $12 < M < 70$ GeV/c^2. No other cuts are imposed.

GeV/c^2. The NLO contributions are dominant over the entire p_T range. The gg channel is the largest, followed closely by the qg channel. Above 80 GeV/c, the LO contribution becomes negligible, even compared to the relatively small NLO $q\bar{q}$ contribution. We note that without the $\langle k_T \rangle$ kick, the LO contribution would die off more rapidly.

Thus heavy quark production is dominated by decay topologies where the Q and $\overline{Q}$ are produced with a light quark or gluon jet in the same hard event. Identification and isolation of these three-prong hard-scattering events would provide a means of selecting the heavy quark production mechanism. Using this criteria, heavy quark propagation can be probed in more detail.

We now turn to a more unique observable: the opening angle between the leptons from semileptonic $D\overline{D}$ and $B\overline{B}$ decays. Figure 3 shows the partonic contributions to $d\sigma/d(\Delta\phi)$ at LO and NLO, as in Fig. 2, with Cut_3 implemented. The LO contribution is strongly peaked back-to-back, appearing only at $\Delta\phi \sim \pi$. Note that the $c\bar{c}$ pairs are more back-to-back due to the lower charm mass and scale. The k_T kick broadens the NLO contributions. Thus the gg and qg NLO $\Delta\phi$ distributions are nearly isotropic due to the presence of the third hard parton in $Q\overline{Q}$+jet events. Angular correlations are then a means of separating the NLO contributions to $Q\overline{Q}$ production.

3.2 Heavy Mesons

We exploit the specific partonic kinematics from Fig. 3 and analyze dileptons from seminleptonic decays of $D\overline{D}$ and $B\overline{B}$. To determine whether the kinematic cuts given in Table 2 can highlight different characteristic $\Delta\phi$ distributions for the $Q\overline{Q}$+jet final state, we show the p_T and $\Delta\phi$ distributions for charm (Fig. 4) and bottom (Fig. 5) decay dileptons with the four kinematic cuts. The p_T distributions are all similar. The bottom rates are somewhat larger than the charm rates, as may be expected [14]. The Cut_4 rate is highest since the $e\mu$ phase space is largest and no mass constraint is applied.

The lepton cuts have the most dramatic effect on the $\Delta\phi$ distributions. The cuts with the lowest minimum dilepton p_T have the highest rate at $\Delta\phi \sim \pi$. The ALICE kinematic regime, with the most restrictive phase space coverage, Cut_1, gives the most back-to-back $\Delta\phi$ distribution. Cut_2, the low p_T CMS dimuon cut, gives a rather isotropic distribution, as does Cut_3, albeit with a lower rate due to the higher p_T cut. Cut_4 exhibits additional structure, with a small back-to-back peak and a larger peak at $\Delta\phi \sim 0$ when the dileptons are almost collinear. Here the jet is back-to-back to the lepton pair. The larger η acceptance enhances detection of topologies where the $Q\overline{Q}$ is opposite the jet, giving a pronounced peak at $\Delta\phi \sim 0$. Thus the reduced η coverage and low minimum p_T of Cut_1 enhances detection of back-to-back lepton pairs. Cut_2 and Cut_3, with larger η coverage, allow more isotropic $Q\overline{Q}X$ final-states to be detected. Indeed, the larger minimum p_T of Cut_3 gives a smaller secondary peak at $\Delta\phi < \pi/2$.

4 Discussion

Since the $Q\overline{Q}$ decay dileptons are opposite the jet at low $\Delta\phi$, we propose to isolate $Q\overline{Q}$+jet events by applying a $\Delta\phi$ cut, $\Delta\phi < 2\pi/3$ or $\Delta\phi < \pi/2$, between $e^{\pm}e^{\mp}$ or $\mu^{\pm}\mu^{\mp}$

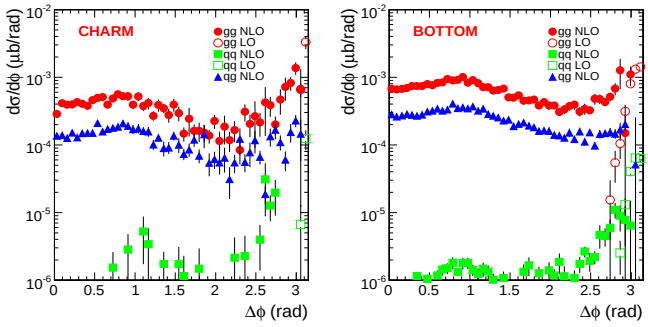

Fig. 3. The same as Fig. 2 for the azimuthal angle between the Q and $\overline{Q}$. Cut_3 has been imposed.

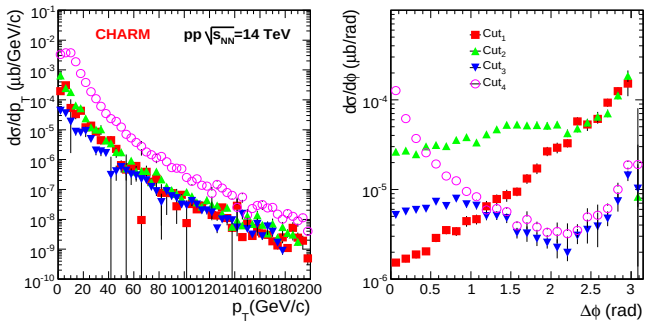

Fig. 4. $D\overline{D}$ meson cut systematics.

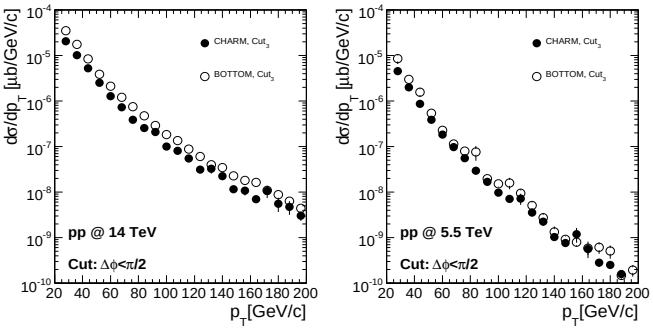

Fig. 6. The dilepton p_T distributions from bottom (solid) and charm (open) decays with Cut_3 and $\Delta\phi < \pi/2$ in pp collisions at 14 TeV (left) and 5.5 TeV (right).

pairs with $12 < M < 70$ GeV/c^2. Since the CMS and ATLAS experiments have symmetric calorimetric and muon identification acceptance, $e^{\pm}e^{\mp}$, $\mu^{\pm}\mu^{\mp}$ and $e^{\pm}\mu^{\mp}$ pairs can be detected. In addition, the invariant mass constraint can be lifted for mixed lepton pairs, $e^{\pm}\mu^{\mp}$, since heavy flavor decays are the only signal source.

While the effect of the $\Delta\phi$ cut can be experimentally investigated with complementary measurements, the width of the p_T distributions in Fig. 2 depends on the intrinsic k_T, especially at low $Q\overline{Q}$ p_T. Since the back-to-back leading order contributions can become more isotropic through the k_T kick, making the additional $\Delta\phi < \pi/2$ cut eliminates this source of contamination.

The dilepton+jet rates as a function of p_T are shown in Fig. 6 for $\sqrt{s} = 14$ and 5.5 TeV, the maximum Pb+Pb energy, using Cut_3 with an additional $\Delta\phi$ cut, $\Delta\phi < \pi/2$. The Pb+Pb rates for the four sets of cuts, assuming a simple A^2 scaling of the pp cross section at $\sqrt{s} = 5.5$ TeV with no energy loss and integrated above a minimum dilepton p_T, p_T^{min}, are shown in Fig. 7. Again, the additional $\Delta\phi$ cut, $\Delta\phi < \pi/2$, is applied.

Following the identification of $Q\overline{Q}$+jet events, the two-body azimuthal correlation between the dilepton and hadrons in the same event can identify the jet and determine its properties. Of course, it may also be possible to fully reconstruct the jet balanced by the dilepton using a jet reconstruction algorithm. The feasibility of these measurements needs further study.

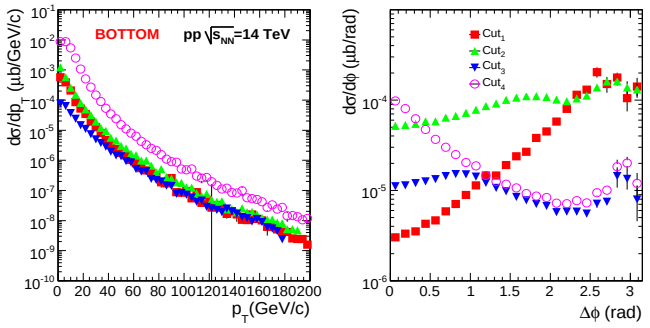

Fig. 5. $B\overline{B}$ meson cut systematics.

While the dileptons from $Q\overline{Q}$ decays are the *signal*, there are several important background sources. The main physics backgrounds are $Z^0/\gamma^* \to l^+l^-$ and $B \to J/\psi X \to l^+l^- X$ decays. There are also *combinatorial* backgrounds from random pairs where one lepton arises from a semileptonic heavy quark decay and another from a light hadron decay, pairs with both leptons from light hadron decays, and pairs of misidentified or fake leptons. These types of background can be reduced using invariant mass cuts, same-sign subtraction ($\mu^{\pm}\mu^{\pm}, e^{\pm}e^{\pm}$), or mixed, opposite-sign dileptons ($e^{\pm}\mu^{\mp}$).

In heavy-ion collisions, there is additional combinatorial background from uncorrelated $c\bar{c}$ and $b\bar{b}$ production since multiple $Q\overline{Q}$ pairs can be produced in the same AA collision. It should be possible to subtract this background by including $Q\overline{Q}$ pairs in the like-sign subtraction scheme. The uncorrelated dileptons not eliminated by the like-sign subtraction will have isotropic azimuthal distributions.

In pp collisions, *pileup* dileptons, from more than one pp collision in a typical bunch crossing, can occur during high luminosity running. However, the excellent vertex reconstruction capabilities of the LHC detectors should minimize the possibility of identifying a fake $Q\overline{Q}$+jet event with the $Q\overline{Q}$ pair from one event and the jet from another event or with each lepton from different events. In heavy-ion collisions, fake dileptons can come from true

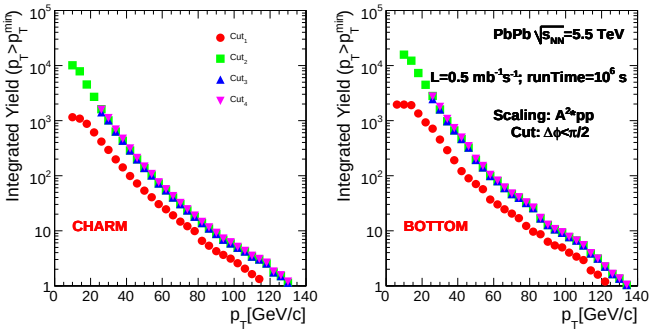

Fig. 7. Integrated bottom (left) and charm (right) rates as a function of p_T^{min} for 5.5 TeV Pb+Pb collisions. No energy loss is included.

heavy meson decays originating from different hard scatterings in one Pb+Pb collision. We estimated the number of $Q\overline{Q}$+jet events in a single Pb+Pb collision at 5.5 TeV to be 0.8 for charm and 1.7 for bottom. The results were obtained by multiplying the *pp* cross section in Fig. 6 by nuclear overlap integral in the 5% most central Pb+Pb collisions, 26.6 mb^{-1} [15]. These backgrounds are rejected if the azimuthal correlation is used for jet identification since a flat distribution is obtained for the fake dileptons.

5 Conclusions

Based on NLO calculations, we proposed a method for identifying $Q\overline{Q}$+jet events both in elementary *pp* collisions and in heavy-ion collisions. The results show that these measurements are feasible at the LHC when jet measurements are combined with judicious dilepton kinematic cuts. High rates are obtained for both the dedicated heavy-ion detector ALICE as well as for the CMS detector with its extended lepton coverage for both muons and electrons.

The type of tagging that we propose is crucial to both the *pp* and *AA* programs since the measurements are related to the heavy-quark production mechanism, the fragmentation functions and medium-induced energy loss.

6 Acknowledgements

This work is supported by the Los Alamos National Laboratory Directed Research and Development grant No. 20060049DR. The work of R. V. was performed under the auspices of the U.S. Department of Energy by Lawrence Livermore National Laboratory under Contract DE-AC52-07NA27344 and NSF grant PHY-0555660.

References

1. B. C. Allanach *et al.*, arXiv:hep-ph/0402295.
2. CMS Collaboration, J. Phys. G **34** (2007) 995; 2807.
3. ATLAS Collaboration, CERN-LHCC-97-22, ATLAS-TDR-10 (1997).
4. B. Alessandro *et al.* [ALICE Collaboration], J. Phys. G **30** (2004) 1517; **32** (2006) 1295.
5. M. Cacciari, P. Nason, and C. Oleary, arXiv:hep-ph/0510032.
6. J. Baines *et al.*, arXiv:hep-ph/0601164v2.
7. I. Vitev, arXiv:hep-ph/08060003.
8. B. I. Abalev *et al.* [STAR Collaboration], Phys. Rev. Lett. **98** (2007) 192301.
9. M. Mangano, P. Nason, and G. Ridolfi, Nucl. Phys. B **373** (1992) 295.
10. C. Peterson *et al.*, Phys. Rev. D **27** (1983) 105.
11. J. Pumplin *et al.*, JHEP **0207** (2002) 012.
12. P. Nason *et al.*, arXiv:hep-ph/0003142.
13. L. Apanasevich *et al.*, Phys. Rev. D **59** (1999) 074007.
14. M. Cacciari, P. Nason, and R. Vogt, Phys. Rev. Lett. **95** (2005) 122001.
15. A. Dainese, N. Carrer, arXiv:hep-ph/0311225.